ADVANCED MATERIALS
www.advmat.de

Revealing the Cooperative Relationship between Spin, Energy, and Polarization Parameters toward Developing High-Efficiency Exciplex Light-Emitting Diodes

Miaosheng Wang, Yi-Hsuan Huang, Kai-Siang Lin, Tzu-Hung Yeh, Jiashun Duan, Tzu-Yu Ko, Shun-Wei Liu, Ken-Tsung Wong,* and Bin Hu**

Experimental studies to reveal the cooperative relationship between spin, energy, and polarization through intermolecular charge-transfer dipoles to harvest nonradiative triplets into radiative singlets in exciplex light-emitting diodes are reported. Magneto-photoluminescence studies reveal that the triplet-to-singlet conversion in exciplexes involves an artificially generated spin-orbital coupling (SOC). The photoinduced electron parametric resonance measurements indicate that the intermolecular charge-transfer occurs with forming electric dipoles ($D^{+\bullet}$→$A^{-\bullet}$), providing the ionic polarization to generate SOC in exciplexes. By having different singlet-triplet energy differences (ΔE_{ST}) in 9,9′-diphenyl-9*H*,9′*H*-3,3′-bicarbazole (BCzPh):3′,3‴,3⁗-(1,3,5-triazine-2,4,6-triyl) tris(([1,1′-biphenyl]-3-carbonitrile)) (CN-T2T) (ΔE_{ST} = 30 meV) and BCzPh:bis-4,6-(3,5-di-3-pyridylphenyl)-2-methyl-pyrimidine (B3PYMPM) (ΔE_{ST} = 130 meV) exciplexes, the SOC generated by the intermolecular charge-transfer states shows large and small values (reflected by different internal magnetic parameters: 274 vs 17 mT) with high and low external quantum efficiency maximum, EQE_{max} (21.05% vs 4.89%), respectively. To further explore the cooperative relationship of spin, energy, and polarization parameters, different photoluminescence wavelengths are selected to concurrently change SOC, ΔE_{ST}, and polarization while monitoring delayed fluorescence. When the electron clouds become more deformed at a longer emitting wavelength due to reduced dipole ($D^{+\bullet}$→$A^{-\bullet}$) size, enhanced SOC, increased orbital polarization, and decreased ΔE_{ST} can simultaneously occur to cooperatively operate the triplet-to-singlet conversion.

Excited states in organic light-emitting diodes (OLEDs) are inevitably formed with both singlets and triplets under electrical excitation. Singlets and triplets are allowed and forbidden to recombine, respectively, due to spin selection rule. It has been shown that the triplets can be almost 100% converted into singlets in thermally activated delayed fluorescence (TADF) molecules based on the design of chemically combining donor and acceptor moieties to enable intramolecular charge-transfer states.[1–4] Recently, various TADF-molecule-based OLEDs with extremely high external quantum efficiency (EQE) exceeding 35% have been successfully demonstrated.[5,6] Similarly, high EQEs can also be conveniently realized by physically mixing donor and acceptor components to form intermolecular charge-transfer states in exciplex systems, where the nonradiative triplets are also largely converted into radiative singlets. The advantages and versatile applications of exciplex systems for giving high-efficiency OLEDs have been highlighted recently.[7] More significantly, OLEDs with exciplex-forming systems as emitting layer have been reported to achieve EQE higher than 19%,[8–10] manifesting their bright and promising prospects in OLED technology based on physically

M. Wang, Prof. B. Hu
Joint Institute for Advanced Materials
Department of Materials Science and Engineering
University of Tennessee
Knoxville, TN 37996, USA
E-mail: bhu@utk.edu

Y.-H. Huang, T.-Y. Ko, Prof. K.-T. Wong
Department of Chemistry
National Taiwan University
and Institute of Atomic and Molecular Science
Academia Sinica, Taipei 10617, Taiwan
E-mail: kenwong@ntu.edu.tw

The ORCID identification number(s) for the author(s) of this article can be found under https://doi.org/10.1002/adma.201904114.

K.-S. Lin, Prof. S.-W. Liu
Department of Electronic Engineering
Ming Chi University of Technology
New Taipei City 24301, Taiwan
E-mail: swliu@mail.mcut.edu.tw

K.-S. Lin, T.-H. Yeh, Prof. S.-W. Liu
Organic Electronics Research Center
Ming Chi University of Technology
New Taipei City 24301, Taiwan

J. Duan
Wuhan National Laboratory for Optoelectronics
Huazhong University of Science and Technology
Wuhan 430074, China

DOI: 10.1002/adma.201904114

 © 2019 WILEY-VCH Verlag GmbH & Co. KGaA, Weinheim

mixing donor and acceptor molecules. The highest EQE of 21.7% has been realized in a 4,4′-cyclohexylidenebis[*N*,*N*-bis(4-methylphenyl)benzenamine] (TAPC):di-[4-(*N*,*N*-ditoly amino)-phenyl] cyclohexane (PIM-TRZ) exciplex OLED very recently.[11] Light-emitting states possess three fundamental parameters: spin, energy, and polarization that essentially govern the triplet-to-singlet conversion. It has been widely demonstrated that a small singlet–triplet energy difference (ΔE_{ST}) is the necessary condition to harvest nonradiative triplets into radiative singlets, providing the basic information on energy parameter effects. On the other hand, spin–orbital coupling (SOC) has been considered as the key mechanism to flip the spins of triplets, enabling the triplet-to-singlet conversion toward developing delayed fluorescence.[12,13] However, the polarization parameter has been reminded as an unaddressed issue to be related to spin and energy parameters (SOC and ΔE_{ST}). In particular, revealing the relationship between these three fundamental parameters (SOC, ΔE_{ST}, and polarization) can provide critical guidelines to design organic light-emitting materials to harvest nonradiative triplets to radiative singlets for further advancing optoelectronic applications.

In this work, we explore the underlying relationship between spin, energy, and polarization parameters based on exciplex systems by using magneto-photoluminescence (magneto-PL), photoinduced electron paramagnetic resonance (EPR), and time-resolved PL measurements. Here, we select two exciplex systems of 9,9′-diphenyl-9*H*,9′*H*-3,3′-bicarbazole (BCzPh):3′,3‴,3⁗⁗-(1,3,5-triazine-2,4,6-triyl)tris(([1,1′-biphenyl]-3-carbonitrile)) (CN-T2T) and BCzPh:bis-4,6-(3,5-di-3-pyridylphenyl)-2-methyl-pyrimidine (B3PYMPM) with high maximum EQE value (EQE_{max}) of 21.05% and low EQE_{max} of 4.89%, respectively, to investigate the relationship between SOC, ΔE_{ST}, and polarization toward harvesting nonradiative triplets into radiative singlets. These two exciplex systems, BCzPh:CN-T2T and BCzPh:B3PYMPM, exhibit similar energy level alignments and thus lead to resembling exciplex emissions, yet different ΔE_{ST} values of 30 and 130 meV, respectively. The SOC was studied by magneto-PL in situ measured on exciplex films. The formation of intermolecular charge-transfer dipoles ($D^{+\bullet}\rightarrow A^{-\bullet}$) was identified by photoinduced EPR characterization. More importantly, by selectively monitoring different PL emission wavelengths, we simultaneously change SOC, ΔE_{ST}, and polarization parameters to study the triplet-to-singlet conversion. Our studies found that increasing polarization through larger deformation of electron clouds, enhancing SOC, and reducing ΔE_{ST} can concurrently occur, establishing a cooperative relationship of spin, energy, and polarization parameters to maximize the triplet-to-singlet conversion through intermolecular charge-transfer states between donor and acceptor molecules in exciplex systems.

Here, we have designed two exciplexes, namely BCzPh:CN-T2T and BCzPh:B3PYMPM (structures shown in **Figure 1**a), where BCzPh[14] serves as an electron donor, and CN-T2T[15] and B3PYMPM[16] serve as electron acceptors. The photophysical behaviors of BCzPh, CN-T2T, and B3PYMPM as well as the BCzPh:CN-T2T and BCzPh:B3PYMPM blends are characterized (Figure S1, Supporting Information). The absorption spectrum of the blend is indeed the superposition of the donor and acceptor absorption. As compared to the emissions of individual components, the donor:acceptor (D:A) blends exhibit significantly redshifted emissions, which are the signature of exciplex formation. The similar emission peaks observed in BCzPh:CN-T2T and BCzPh:B3PYMPM blends are consistent with the energy level alignments of these two exciplex systems as shown in Figure 1b. The characteristics of these two corresponding exciplex OLEDs with the same device structure of indium tin oxide (ITO)/1,4,5,8,9,11-hexaazatriphenylene hexacarbonitrile (HATCN) (10 nm)/TAPC (35 nm)/BCzPh (10 nm)/exciplex layer (D:A = 1:1; 25 nm)/CN-T2T (40 nm)/lithium fluoride (LiF) (1 nm)/aluminum (Al) (100 nm) are examined. The electroluminescence (EL) spectra of these two devices based on BCzPh:CN-T2T and BCzPh:B3PYMPM exciplexes shown in Figure 1c indicate that there is no emission from either donor or acceptor. The device based on BCzPh:CN-T2T exciplex demonstrates a low turn-on voltage of 2.4 V and a maximum luminance (L_{max}) of 10 655 cd m^{-2} at 8 V (35.65 mA cm^{-2}) (Figure 1d). More importantly, the BCzPh:CN-T2T exciplex OLED exhibits the EQE_{max} reaching 21.05% which still retains a large value of 16.85% at high luminance of 1000 cd m^{-2} (Figure 1e). This is the one of the highest performances among all exciplex OLEDs. The high EQE implies that nonradiative triplets have been largely converted into radiative singlets in BCzPh:CN-T2T exciplex OLED. The power dependence of the emission shows a slope value close to 1, indicating that the triplet-to-singlet conversion comes from TADF rather than triplet–triplet annihilation (Figure S2, Supporting Information).[17] In sharp contrast, with the same device structure, the BCzPh:B3PYMPM exciplex-based device shows a low EQE_{max} of 4.89% with a higher turn-on voltage of 2.5 V and a lower L_{max} of 664 cd m^{-2} at 8 V (23.41 mA cm^{-2}). Detailed device parameters of the BCzPh:CN-T2T and BCzPh:B3PYMPM based exciplex OLEDs are presented in Table S1 (Supporting Information). Note that the effect of charge balance is one of most key issues to determine the OLED device performance.[15,18] Here, as shown in Figure S3 (Supporting Information), carrier mobilities in both exciplexes have the same order of magnitude ($\approx 10^{-5}$ cm^2 V^{-1} S^{-1}). Moreover, these two exciplex systems have same donor (BCzPh) and acceptors with similar lowest unoccupied molecular orbital (LUMO) and highest occupied molecular orbital (HOMO) (2.7 and 6.7 eV for CN-T2T vs 2.8 and 6.8 eV for B3PYMPY). Therefore, our two selected exciplex systems should have similar balanced injection of carriers. Furthermore, the PL quantum yields (PLQY) of BCzPh:CN-T2T and BCzPh:B3PYMPM blends are measured to be 63.7% and 30.2%, respectively. The PLQY are different by about a factor of 2 in BCzPh:CN-T2T and BCzPh:B3PYMPM exciplexes. But, the EQE values are different by a factor of 4. Therefore, it is obvious that the BCzPh:CN-T2T exciplex undergoes a stronger spin mixing to efficiently harvest the triplets in comparison with BCzPh:B3PYMPM exciplex. However, the underlying factors that lead to such a considerable difference between these two blends with similar energy level alignments (Figure 1b) are unclear. Therefore, it becomes an urgent need to explore the detailed mechanism to operate delayed fluorescence in exciplex states by considering spin, energy, and polarization parameters.

Previous studies have concluded that decreasing the ΔE_{ST} value can facilitate the spin mixing to convert triplets to singlets. However, the effect of ΔE_{ST} on spin mixing can be validated only if the spin-flipping mechanism is existed. It is commonly recognized that the SOC can function as the primary mechanism

© 2019 WILEY-VCH Verlag GmbH & Co. KGaA, Weinheim

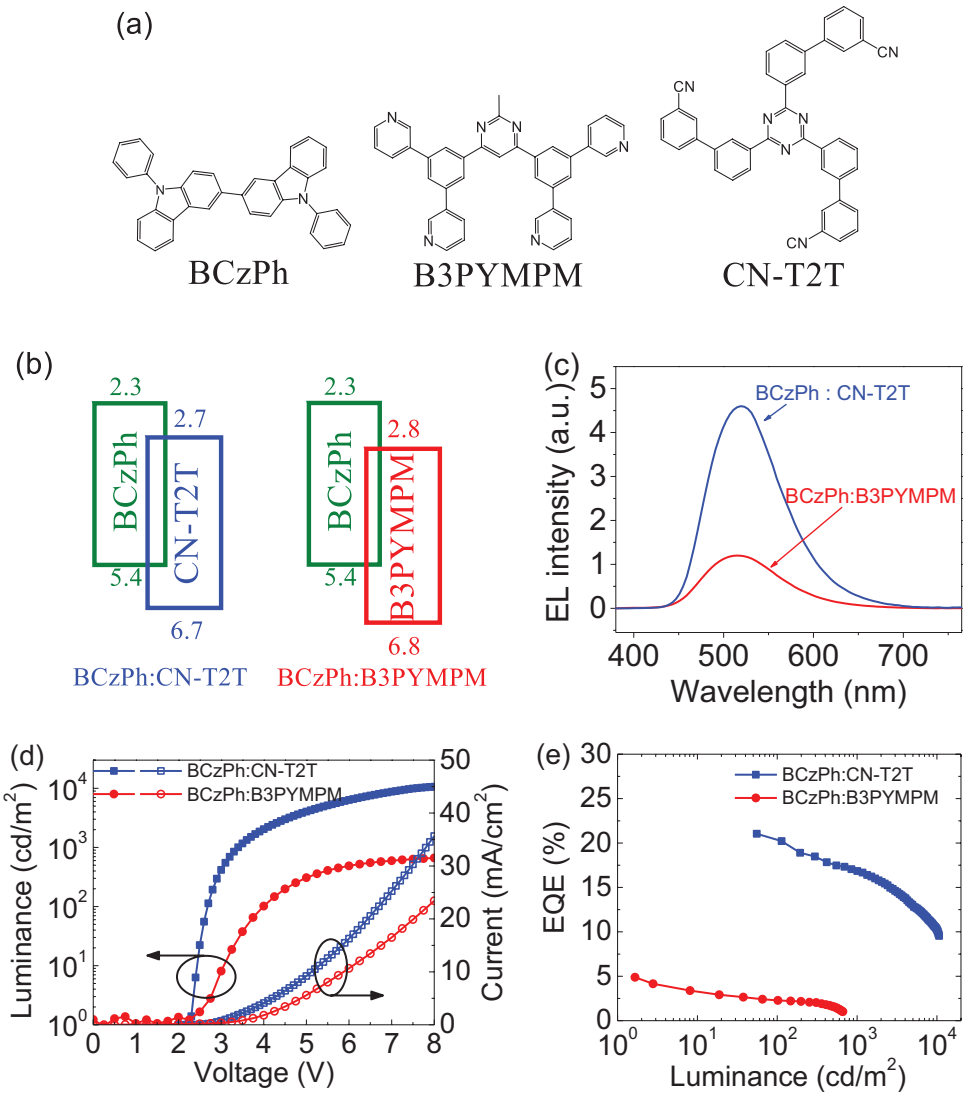

Figure 1. Device characterization for BCzPh:CN-T2T and BCzPh:B3PYMPM exciplex OLEDs. a) Molecular structures of BCzPh, B3PYMPM, and CN-T2T. b) Energy diagram of the exciplexes. c) EL spectra of the two exciplex OLEDs with the same device structure: ITO/HATCN (10 nm)/TAPC (35 nm)/BCzPh (10 nm)/exciplex layer/CN-T2T (40 nm)/LiF (1 nm)/Al (100 nm) at 3.5 V bias. d) Current–voltage–luminance characteristics. e) EQE as the function of luminance.

to enable spin flipping toward spin mixing, as exampled in phosphorescent complex with heavy metal.[19,20] Indeed, SOC as the spin-flipping mechanism in D–A type TADF molecules has been recently admitted,[21] in contrast with the early results where hyperfine interaction (HFI) is considered as the spin-flipping mechanism.[3] However, until now there is still in short of experimental evidence to directly prove the SOC effects in exciplex systems with efficient delayed fluorescence.

Now, we use magneto-PL, as an in situ method, to explore the underlying mechanism responsible for the spin mixing in exciplex OLEDs. In general, magneto-PL can occur when an external magnetic field changes the intersystem crossing through the spin-flipping mechanism with the consequence of changing the populations on singlet and triplet states.[22,23] Essentially, an external magnetic field can compete with HFI or SOC to change the intersystem crossing between singlet and triplet states, leading to a magneto-PL occurring in low (<10 mT, HFI)[24,25] and high (>10 mT, SOC) fields,[26–28] respectively. Therefore, magneto-PL can reveal two critical information in exciplexes: i) whether spin flipping is occurred and ii) whether the spin flipping is governed by HFI or SOC. As shown in **Figure 2**a, both BCzPh:CN-T2T and BCzPh:B3PYMPM exciplexes exhibit a magneto-PL at high field (>10 mT). This high-field magneto-PL indicates that there surprisingly exists an SOC in both BCzPh:CN-T2T and BCzPh:B3PYMPM exciplex systems with higher and lower values as shown by the larger and smaller internal magnetic parameters (B_0 = 274 mT vs B_0 = 17 mT). Generally, it has been known that SOC requires a heavy element in organic materials.[29,30] Because the exciplex systems do not have any heavy element, the SOC revealed by our magneto-PL indicates that there exists a new mechanism to generate an artificial SOC to realize the spin flipping toward

© 2019 WILEY-VCH Verlag GmbH & Co. KGaA, Weinheim

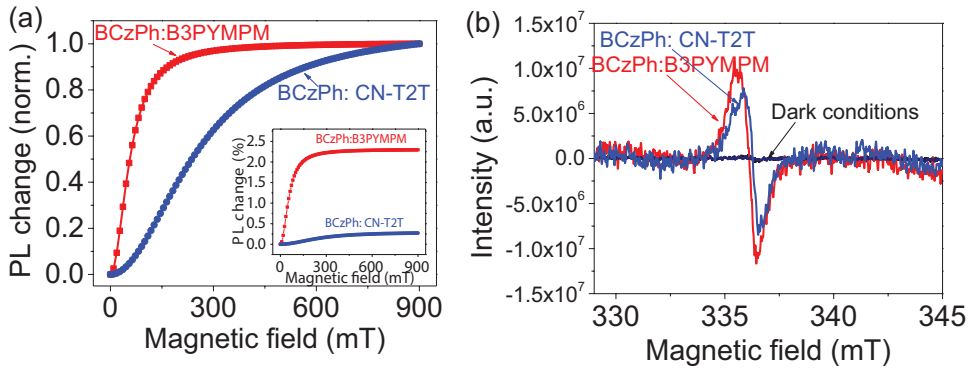

Figure 2. a) Normalized magneto-PL for BCzPh:CN-T2T and BCzPh:B3PYMPM exciplex thin films; the inset shows the original magneto-PL signals. b) EPR signals for BCzPh:CN-T2T and BCzPh:B3PYMPM exciplex thin films under dark and 405 nm photoexcitation conditions.

harvesting the nonradiate triplets for developing high-efficiency OLEDs. Clearly, a stronger SOC provides a more effective spin flipping to harvest the nonradiative triplets into radiative singlets, providing the necessary condition to develop high-efficiency exciplex OLEDs.

To understand the origin of SOC in exciplexes, we consider that the donor and acceptor molecules become positively and negatively charged ions ($D^{+\bullet}$ and $A^{-\bullet}$) through the intermolecular charge-transfer process in an exciplex system under photoexcitation, leading to an optically induced dipole $D^{+\bullet}\rightarrow A^{-\bullet}$. Before exciting molecules, the D and A molecules have negligible SOC due to isotropic orbital wavefunctions. When optically induced dipole $D^{+\bullet}\rightarrow A^{-\bullet}$ is formed with ionic polarization in an exciplex, the isotropic orbitals can be asymmetrically polarized due to Coulombic attraction between $D^{+\bullet}$ and $A^{-\bullet}$, providing the necessary condition to form an SOC through the interaction between asymmetrically polarized orbitals and spins. Here, the polarization refers to the deformation of electron clouds on $D^{+\bullet}$ and $A^{-\bullet}$ within an exciplex in excited state. A larger deformation of electron clouds means a stronger polarization, leading to a higher SOC. Therefore, the photoinduced $D^{+\bullet}\rightarrow A^{-\bullet}$ dipoles function as the critical parameter responsible for generating an SOC in exciplexes. Here, the EPR is employed to indicate the charged ions with the consequence of forming intermolecular charge-transfer states in exciplexes under photoexcitation. As shown in Figure 2b, both BCzPh:CN-T2T and BCzPh:B3PYMPM films demonstrate a strong EPR signal under photoexcitation, while the dark condition shows a negligible signal. This photoinduced EPR signals provide evidence to show the formation of optically generated ions within exciplex systems. It is noted that the observation of optically generated ions in our exciplex systems is consistent with the recently observed photoinduced polarons by using transient infrared absorption in an D:A (CN-Cz2:PO-T2T) exciplex.[31] This result confirms that the charge transfer between the donor and acceptor indeed occurs and consequently leads to the formation of optically induced dipoles ($D^{+\bullet}\rightarrow A^{-\bullet}$) toward developing an artificial SOC in exciplex systems.

Essentially, the SOC enabled by the optically induced dipoles decides whether the spin flipping can occur between singlet and triplet states in exciplexes. As exampled in fluorescent and phosphorescent molecules, the spin flipping becomes forbidden and allowed, regardless of singlet–triplet energy difference, when SOC is absent and present, respectively. In the absence of SOC, when the HFI initiates a low-degree spin flipping, the spin mixing between singlets and triplets can be increased by thermal energy in aromatic molecules.[32] When the SOC is established to allow the spin flipping, the spin mixing between singlets and triplets can be essentially controlled by the ΔE_{ST} to harvest nonradiative triplets into radiative singlets. Empirically, the spin mixing rate (λ) can be simply expressed as $\lambda = H_{SO}/\Delta E_{ST}$, where H_{SO} and ΔE_{ST} are the SOC constant and energy difference between S_1 and T_1 states.[33] Here, we explore the relationship between spin, energy, and polarization parameters by simultaneously changing SOC, ΔE_{ST}, and polarization through detecting the PL from short to long wavelength while monitoring the delayed fluorescence to show triplet-to-singlet conversion. Moving the PL detection from short to long wavelength corresponds to decreasing the D:A distance, consequently increasing the polarization with enhanced deformation of electron clouds on $D^{+\bullet}$ and $A^{-\bullet}$ due to Coulombic attraction. At shorter emitting wavelength (higher energy), the optically induced dipole ($D^{+\bullet}\rightarrow A^{-\bullet}$) has a longer separation distance (larger dipole moment), leading to a less deformation of electron clouds on $D^{+\bullet}$ and $A^{-\bullet}$ and a weaker SOC. In this situation, the ΔE_{ST} is also large. At a longer emitting wavelength (lower energy), the optically induced dipole ($D^{+\bullet}\rightarrow A^{-\bullet}$) has a shorter separation distance (smaller dipole moment), generating more deformation of electron clouds on $D^{+\bullet}$ and $A^{-\bullet}$ and a stronger SOC. In this situation, the ΔE_{ST} becomes smaller. It has been observed that decreasing the D:A distance leads to a reduced ΔE_{ST} with increased formation of intermolecular charge-transfer states upon moving PL detection from short to long wavelength.,[34,35] Therefore, detecting the PL from short to long wavelength provides a vital method to explore the relationship between spin, energy, and polarization parameters toward harvesting nonradiative triplets into radiative singlets by simultaneously monitoring magneto-PL and time-resolved PL. **Figure 3**a shows the PL spectrum of the high-efficiency BCzPh:CN-T2T exciplex system under 375 nm continuous-wave (CW) laser excitation. It is obvious that the magneto-PL line-width for the high-efficiency BCzPh:CN-T2T exciplex system gradually increases as moving the PL detection from short to longer wavelength (Figure 3b), increasing the internal magnetic parameter B_0 from 214 mT (at the shorter PL wavelength of 480 nm) to 312 mT (at the longer PL wavelength

© 2019 WILEY-VCH Verlag GmbH & Co. KGaA, Weinheim

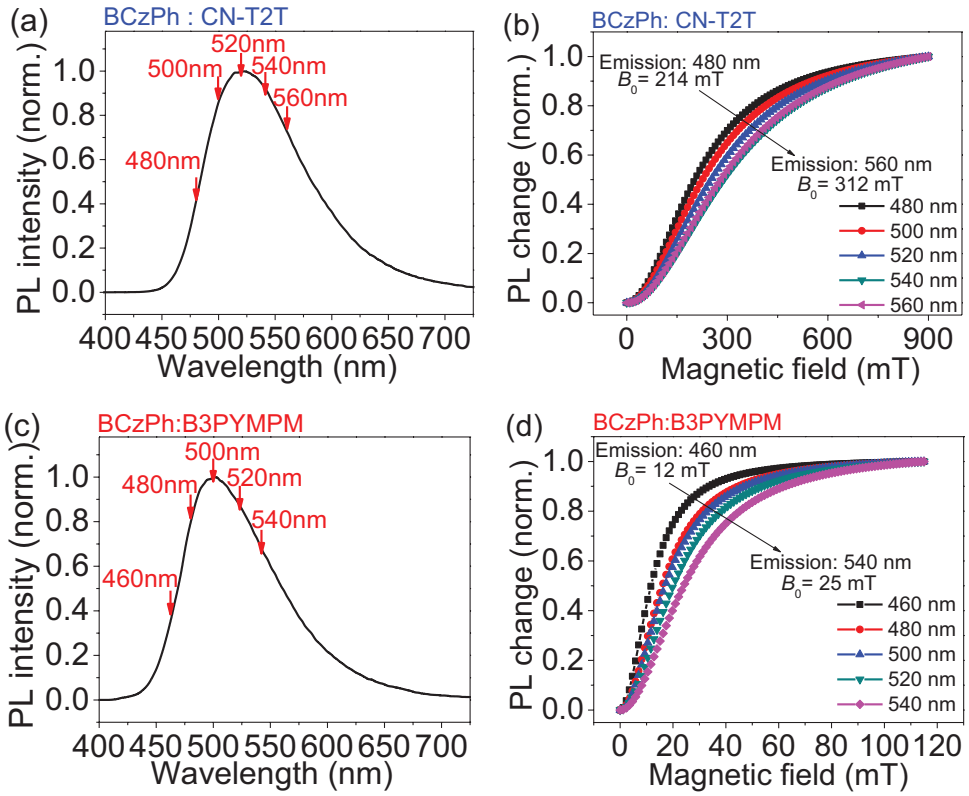

Figure 3. PL spectra and emission wavelength dependent magneto-PL. a) PL spectrum of BCzPh:CN-T2T exciplex. b) Wavelength-dependent magneto-PL of BCzPh:CN-T2T exciplex. c) PL spectrum of BCzPh:B3PYMPM exciplex. d) Wavelength-dependent magneto-PL of BCzPh:B3PYMPM exciplex.

of 520 nm). The low-efficiency exciplex BCzPh:B3PYMPM system shows a similar phenomenon: the B_0 value increases from 12 to 25 mT upon moving the PL detection from short (460 nm) to long (500 nm) wavelengths (Figure 3c,d). Clearly, we can see that decreasing the dipole ($D^{+\bullet}\rightarrow A^{-\bullet}$) distance corresponds to the enhanced Coulombic attraction between $D^{+\bullet}$ and $A^{-\bullet}$, consequently increasing SOC according to wavelength-dependent magneto-PL. Moreover, we can expect that moving the PL detection from short to long wavelength corresponds to the reduced ΔE_{ST}.[35] Simultaneously, moving the PL detection from short to long wavelength largely increases the delayed fluorescence, as shown in **Figure 4**. The fitting parameters on the wavelength-dependent PL decay curves are presented in Tables S2 and S3 (Supporting Information) for BCzPh:CN-T2T and BCzPh:B3PYMPM exciplexes, respectively. This serves as the first evidence to show the cooperative relationship between spin, energy, and polarization parameters to maximally harvest nonradiative triplets into radiative singlets toward developing high-efficiency OLEDs through intermolecular charge-transfer states in exciplex systems.

Now we discuss the enhanced horizontal orientation of transition dipoles occurring in exciplex systems. It is well known that, with enhanced horizontal orientation of optical transition dipoles, the light outcoupling can be more

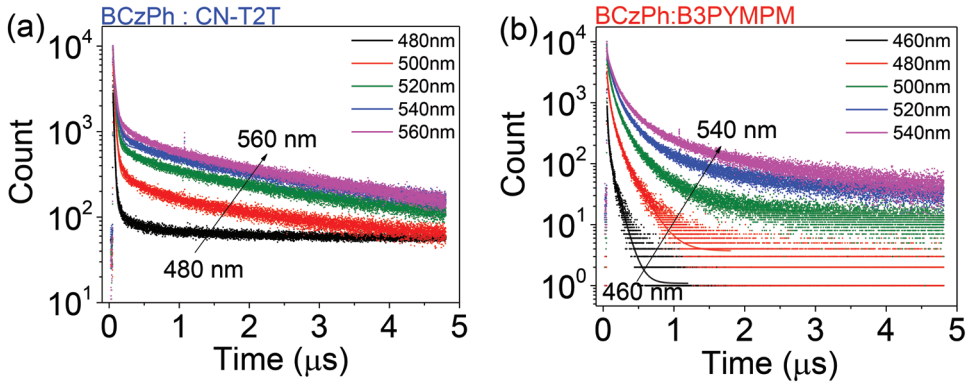

Figure 4. a,b) Emission wavelength dependent PL decay curves of BCzPh:CN-T2T (a) and BCzPh:B3PYMPM (b) exciplex thin films.

© 2019 WILEY-VCH Verlag GmbH & Co. KGaA, Weinheim

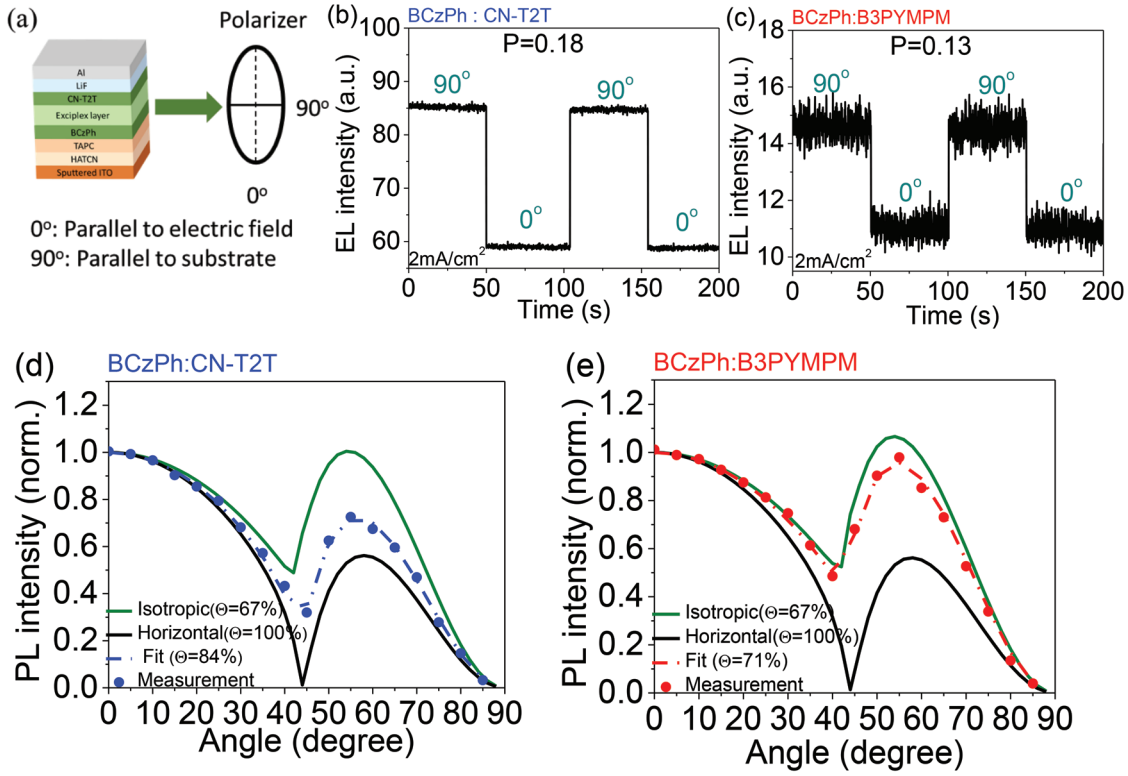

Figure 5. Transient dipole direction measurements for both EL and PL. a) Experimental setup diagram to show the polarized EL measurement in exciplex OLEDs from the near-parallel direction with the device plane. b) Polarization-resolved EL for BCzPh:CN-T2T exciplex OLED. c) Polarization-resolved EL for BCzPh:B3PYMPM exciplex OLED. The polarization ratio is defined by $P = \frac{EL_{90^\circ} - EL_{0^\circ}}{EL_{90^\circ} + EL_{0^\circ}}$. d,e) p-Polarized PL intensity (at PL peak wavelength) of different emitting layers as a function of the emission angle for BCzPh:CN-T2T and BCzPh:B3PYMPM exciplex thin films. The measured curves are compared to simulated curves with different horizontal dipole ratios Θ to extract the horizontal emitting dipole ratios of different emitting layers.

efficient to develop high EQEs in OLEDs.[5,36] Here, the orientations of light-emitting states of these two exciplexes are characterized by using polarization-dependent EL, as shown in **Figure 5**a. The polarization-resolved EL is monitored from the near-parallel direction to the device plane. The EL with the polarization at parallel direction to the device plane (90°) is generated by horizontally orientated in-plane emitting dipoles, while the EL at perpendicular direction to the device plane (0°) comes from out-of-plane emitting dipoles. The BCzPh:CN-T2T and BCzPh:B3PYMPM OLEDs exhibit larger and smaller $\frac{EL_{90^\circ} - EL_{0^\circ}}{EL_{90^\circ} + EL_{0^\circ}}$ ratios (18% vs 13%), respectively. In addition, the angle-dependent PL measurements shown in Figure 5d,e confirm that the light-emitting states become more horizontally oriented in high-efficiency (BCzPh:CN-T2T) exciplex (Θ = 84%) as compared to low-efficiency (BCzPh:B3PYMPM) exciplex (Θ = 71%). Based on this observation, we can speculate that stronger charge-transfer characteristics caused by larger difference in electronegativity between donor and acceptor molecules can lead to more horizontally oriented optical transition dipoles in exciplex systems. When co-evaporating D and A molecules on substrate, the D and A molecules can form aggregations to generate D:A exciplexes. The high Θ value in the BCzPh:CN-T2T exciplex system suggests that aggregated D and A molecules can have asymmetric shapes: more preferably on horizontal direction and less preferably on vertical direction due to space-limited vertical aggregation within a thin film. As a consequence, the aggregated D and A molecules have higher probability to form exciplexes in the horizontal direction relative to vertical direction in the high-efficiency BCzPh:CN-T2T system. The enhanced horizontal orientation of light-emitting states in BCzPh:CN-T2T exciplex system due to stronger intermolecular D:A interaction can increase the EQE through increased light outcoupling efficiency.

In summary, our studies revealed the cooperative relationship between spin, energy, and polarization parameters to harvest nonradiative triplets into radiative singlets toward developing high-efficiency OLEDs based on two selected exciplex systems (BCzPh:CN-T2T and BCzPh:B3PYMPM). The magneto-PL signal in high field (>10 mT) provides the direct evidence that high-efficiency BCzPh:CN-T2T and low-efficiency BCzPh:B3PYMPM exciplex systems are formed with high and low SOC values, reflected largely by different internal magnetic parameters ($B_0 \approx 274$ mT vs $B_0 \approx 17$ mT). The EPR results indicate that the photoinduced charge transfer leads to optically generated ions ($D^{+\bullet}$ and $A^{-\bullet}$) to form charge-transfer dipoles ($D^{+\bullet} \rightarrow A^{-\bullet}$), thus providing the necessary condition to generate an SOC by asymmetrically polarizing orbital wavefunctions in exciplex states. By moving the PL detection from short to long wavelength to probe the charge-transfer dipoles ($D^{+\bullet} \rightarrow A^{-\bullet}$) with long and short separation distances, we found that the SOC is increased while the ΔE_{ST} is decreased with the consequence

© 2019 WILEY-VCH Verlag GmbH & Co. KGaA, Weinheim

of boosting the delayed fluorescence in exciplex systems. This presents a cooperative relationship between spin, energy, and polarization parameters through intermolecular charge-transfer states to operate the triplet-to-singlet conversion toward enhancing delayed fluorescence in exciplex systems. Furthermore, we observed that light-emitting states in high-efficiency BCzPh:CN-T2T exciplex OLED are more horizontally orientated in film plane, increasing light outcoupling efficiency toward high EQE. This indicates that using D:A exciplex design provides an important approach to increase the horizontal orientation ratio of transition dipoles through space-limited aggregation of D and A molecules in vertical direction during thin-film formation. The preferred horizontal orientation of transient dipoles can increase the light extraction in exciplex OLEDs. Therefore, our studies show that spin, energy, and polarization parameters cooperatively operate the triplet-to-singlet conversion with more horizontally oriented transition dipoles toward increasing delayed fluorescence and EQE, providing a critical guideline to further advance the developments of OLEDs.

Experimental Section

Materials and Devices: The organic and inorganic materials, including the HATCN, TAPC, BCzPh, B3PYMPM, LiF, and Al, were purchased from Shine Materials Technology Co., Ltd. In addition to such organic materials, the CN-T2T was synthesized in the laboratory following previous work.[15] Before the device preparation, all organic materials were sublimated twice through the homemade graded purification system with a high vacuum level of 8×10^{-6} Torr. For substrate preparation, the glass substrate was cleaned using acetone and isopropyl alcohol in an ultrasonic bath and blowing dry with nitrogen gas. Then, a sputtered ITO film of 80 nm was deposited on a glass substrate and defined the pixel size by the laser patterning method.[37] After ITO substrate's preparation, the OLED fabrication process was carried out by the thermal evaporation system under a high vacuum level of 2×10^{-6} Torr, which deposited organic thin films on the substrate. For the deposition process, each organic thin film was conducted with a constant rate of ≈0.5 Å s^{-1} and monitored by an in situ quartz crystal. The active area of 4 mm^2 was defined by anode and cathode pad's overlapped region. After the device fabrication process, the devices were transferred into a nitrogen-filled glovebox (oxygen, moisture < 0.1 ppm) for preparing the encapsulation process with UV-curable epoxy resin (Everwide Chemical Corporation Limited EXC345) and getter-attached cover glass to protect the OLED devices. In this work, the exciplex OLED devices were fabricated following two standard structures: ITO/HATCN (10 nm)/TAPC (35 nm)/BCzPh (10 nm)/exciplex layer (mixture ratio of 1:1)/CN-T2T (40 nm)/LiF (1 nm)/Al (100 nm), while the emissive layer (EML) was prepared with both exciplex emitters of the BCzPh: CN-T2T and BCzPh: B3PYMPM for comparison. All testing thin films in the photophysical studies were deposited on the quartz substrates by using a thermal evaporator under a high vacuum of 5×10^{-6} Torr. The deposition rate was fixed at 0.5 Å s^{-1}, while the thin-film thickness was 80 nm for each testing sample. The fabrication process of the space charge limiting current (SCLC) sample was similar to OLEDs, as mentioned in the part of device preparation. The hole-only structure was ITO/MoO_3 (6 nm)/C_{60} (3 nm)/BCzPh:CN-T2T (150 nm) and BCzPh:B3PYMPM (50 nm)/C_{60} (3 nm)/MoO_3 (10 nm)/Al (100 nm), where the buffer layer of C_{60} can provide an efficient hole injection for deep HOMO level of hole-transporting materials.[38] On the other hand, the structure of electron-only device was ITO/BPhen: 20 wt% CS_2CO_3 (5 nm)/BCzPh:CN-T2T (150 nm), and BCzPh:B3PYMPM (50 nm)/LiF (1 nm)/Al (100 nm). In the previous work, it was found that the buffer layer of BPhen:CS_2CO_3 can easily reduce the injection barrier between the ITO and organic layer's LUMO to provide efficient electron injection efficiency.[39] Therefore, the BPhen:CS_2CO_3 is a suitable buffer layer, which deposited on the ITO acting as electron-only device's anode electrode. Electrical characterization was measured by the Keithley 2400 source meter, while the device processed the encapsulation in the nitrogen-filled glove box to avoid any degradation issue in the ambient.

Characterizations: The current density–voltage–luminance (*J*–*V*–*L*) characteristics and emission spectrum of the proposed devices were measured by a HORIBA Fluorolog-3 spectrometer combined with a source meter (Keithley 2400), which was controlled by LabVIEW program. The integrated sphere system (SLM-6Z, Isuzu optics) was used to evaluate the EQE value of the OLEDs in ambient condition. The magneto-PL signals were measured by monitoring the PL intensity as a function of magnetic field at room temperature. The magneto-PL amplitude is defined as $\mathrm{MFE} = \frac{I_B - I_0}{I_0}$, where I_B and I_0 are the PL intensities with and without an external magnetic field. The Lorentzian function $\left(\mathrm{MFE} = \alpha \frac{B^2}{B^2 - B_0^2}\right)$ was used to fit the magneto-PL curves, where B_0 represent the internal magnetic parameter. The PL intensities and spectra were measured by using HORIBA Fluorolog-3 spectrometer. PL decay curves were measured by using the Time Correlated Single Photon Counting System (TCSPC) in HORIBA Fluorolog-3 spectrometer with nanosecond pulsed light excitation from a nanoLED (375 nm). The fitting of PL decay curves was conducted by using the DAS6 fluorescence decay analysis software from HORIBA. The EPR measurements were performed on a Bruker EPR A300 machine (X band). For the absorption measurement, the thin-film samples were measured by using a UV–vis spectrophotometer (Thermo Scientific Evolution 220). The thin-film samples, BCzPh:CN-T2T and BCzPh:B3PYMPM, were measured by using a nitrogen-filled integrating sphere (Quanta-ϕ, HORIBA Jobin Yvon) for an absolute PLQY measurement. Note that the testing of samples was conducted using an ozone-free xenon arc lamp with the excitation source of 305 nm with a pulse frequency of 50 kHz and a power density of $\approx 87 \times 10^{-6}$ W m^{-2}. To evaluate the ΔE_{ST} of these two exciplex thin-film samples, the PL spectra (fluorescence and phosphorescence) were recorded with a spectrofluorometer (FluoroMax Plus, HORIBA Jobin Yvon) with an excitation wavelength of 305 nm (150 W ozone-free xenon arc lamp) in the nitrogen-filled chamber. For fluorescence measurement, the organic thin-film samples were placed in the sample holder and without setting delay time for characterization. On the other hand, for phosphorescence measurement, the samples were measured at low temperature (77 K) in the system's liquid nitrogen holder, while the delay time was set to 2 ms for PL spectrum measurement. Note that such analysis was similar to previous works as relative to the efficient exciplex OLEDs.[40–42] For the analysis of the transition dipole orientation of exciplex emitters, the experimental setup was followed by previous work.[36,43] This measurement system included a fused silica-based half-cylindrical lens with a testing sample, a precise motorized rotation stage, a fiber-guided spectrometer (USB 4000, Ocean Optics) with a polarizer and long pass filter to collect the polarized emission. Regarding the such measurement system's excitation source, a CW neodymium-doped yttrium aluminum garnet (Nd:YAG) laser (355 nm, 10 kHz) was used to excite the samples with an incident angle of 45°. For the collection of the intensity of the p-polarized emission, the spectrometer with the LabVIEW program recorded various PL intensity from 0° to 90° with the step of 5°. To compare the measurement result, SETFOS 4.5 (Fluxim AG, Switzerland) was used to plot the simulation data and to fit the ratio of horizontal dipoles (Θ). Note that the tris-(8-hydroxyquinoline) aluminum with a completely random orientation of Θ ≈ 0.66 was used to calibrate this measurement system. Such a testing procedure was similar to the previous work.[44] The SCLC measurements were conducted by the Keithley 2400 source meter, which was followed by previous work to determine the charge mobility of organic semiconducting materials with a thin thickness less than 200 nm.[18,45] To estimate the value of carrier mobility (μ), the hole- and electron-only devices were characterized by the well-known Mott–Gurney SCLC equation, as shown below

$$J = \frac{9}{8} \varepsilon \varepsilon_0 \mu \frac{V^2}{d^3} \quad (1)$$

© 2019 WILEY-VCH Verlag GmbH & Co. KGaA, Weinheim

where J is the device's current density, ε is the relative permittivity of a material, ε_0 is the permittivity of vacuum, V is the applied voltage, and d is the active thickness of the thin film.

Supporting Information

Supporting Information is available from the Wiley Online Library or from the author.

Acknowledgements

The authors at University of Tennessee acknowledge the funding supports from Air Force Office of Scientific Research (AFOSR) under the grant number FA 9550-15-1-0064, AOARD (FA2386-15-1-4104), and National Science Foundation (NSF-1911659). The authors in Taiwan were supported with the funding from the Ministry of Science and Technology Taiwan (107-2113-M-002-019-MY3, 107-2119-M-131-001).

Conflict of Interest

The authors declare no conflict of interest.

Keywords

charge-transfer states, delayed fluorescence, exciplexes, orbital polarization, spin–orbital coupling

Received: June 28, 2019
Revised: September 6, 2019
Published online:

[1] Y. Liu, C. Li, Z. Ren, S. Yan, M. R. Bryce, *Nat. Rev. Mater.* **2018**, *3*, 18020.
[2] Y. Tao, K. Yuan, T. Chen, P. Xu, H. Li, R. Chen, C. Zheng, L. Zhang, W. Huang, *Adv. Mater.* **2014**, *26*, 7931.
[3] T. Ogiwara, Y. Wakikawa, T. Ikoma, *J. Phys. Chem. A* **2015**, *119*, 3415.
[4] S. Jeon, H. Lee, K. Yook, J. Lee, *Adv. Mater.* **2019**, *31*, 1803524.
[5] T. A. Lin, T. Chatterjee, W. L. Tsai, W. K. Lee, M. J. Wu, M. Jiao, K. C. Pan, C. L. Yi, C. L. Chung, K. T. Wong, *Adv. Mater.* **2016**, *28*, 6976.
[6] D. H. Ahn, S. W. Kim, H. Lee, I. J. Ko, D. Karthik, J. Y. Lee, J. H. Kwon, *Nat. Photonics* **2019**, *13*, 540.
[7] M. Sarma, K.-T. Wong, *ACS Appl. Mater. Interfaces* **2018**, *10*, 19279.
[8] M. Colella, A. Danos, A. P. Monkman, *J. Phys. Chem. Lett.* **2019**, *10*, 793.
[9] D. H. Ahn, H. Lee, S. W. Kim, D. Karthik, J. Lee, H. Jeong, J. Y. Lee, J. H. Kwon, *ACS Appl. Mater. Interfaces* **2019**, *11*, 14909.
[10] M. Chapran, P. Pander, M. Vasylieva, G. Wiosna-Salyga, J. Ulanski, F. B. Dias, P. Data, *ACS Appl. Mater. Interfaces* **2019**, *11*, 13460.
[11] B. Liang, J. Wang, Z. Cheng, J. Wei, Y. Wang, *J. Phys. Chem. Lett.* **2019**, *10*, 2811.
[12] M. K. Etherington, J. Gibson, H. F. Higginbotham, T. J. Penfold, A. P. Monkman, *Nat. Commun.* **2016**, *7*, 13680.
[13] H. Noda, X.-K. Chen, H. Nakanotani, T. Hosokai, M. Miyajima, N. Notsuka, Y. Kashima, J.-L. Brédas, C. Adachi, *Nat. Mater.* **2019**, *18*, 1084.
[14] H. Sasabe, N. Toyota, H. Nakanishi, T. Ishizaka, Y. J. Pu, J. Kido, *Adv. Mater.* **2012**, *24*, 3212.
[15] W.-Y. Hung, P.-Y. Chiang, S.-W. Lin, W.-C. Tang, Y.-T. Chen, S.-H. Liu, P.-T. Chou, Y.-T. Hung, K.-T. Wong, *ACS Appl. Mater. Interfaces* **2016**, *8*, 4811.
[16] D. Tanaka, H. Sasabe, Y.-J. Li, S.-J. Su, T. Takeda, J. Kido, *Jpn. J. Appl. Phys.* **2007**, *46*, L10.
[17] F. B. Dias, T. J. Penfold, A. P. Monkman, *Methods Appl. Fluoresc.* **2017**, *5*, 012001.
[18] N. B. Kotadiya, P. W. M. Blom, G.-J. A. H. Wetzelaer, *Nat. Photonics* **2019**, https://doi.org/10.1038/s41566-019-0488-1.
[19] M. A. Baldo, D. O'brien, Y. You, A. Shoustikov, S. Sibley, M. Thompson, S. R. Forrest, *Nature* **1998**, *395*, 151.
[20] M. Baldo, M. Thompson, S. Forrest, *Nature* **2000**, *403*, 750.
[21] E. W. Evans, Y. Olivier, Y. Puttisong, W. K. Myers, T. J. Hele, S. M. Menke, T. H. Thomas, D. Credgington, D. Beljonne, R. H. Friend, *J. Phys. Chem. Lett.* **2018**, *9*, 4053.
[22] H. Xu, M. Wang, Z.-G. Yu, K. Wang, B. Hu, *Adv. Phys.* **2019**, *68*, 49.
[23] S. Baniya, Z. Pang, D. Sun, Y. Zhai, O. Kwon, H. Choi, B. Choi, S. Lee, Z. V. Vardeny, *Adv. Funct. Mater.* **2016**, *26*, 6930.
[24] T. D. Nguyen, G. Hukic-Markosian, F. Wang, L. Wojcik, X.-G. Li, E. Ehrenfreund, Z. V. Vardeny, *Nat. Mater.* **2010**, *9*, 345.
[25] P. Bobbert, T. Nguyen, F. Van Oost, v. B. Koopmans, M. Wohlgenannt, *Phys. Rev. Lett.* **2007**, *99*, 216801.
[26] B. Hu, L. Yan, M. Shao, *Adv. Mater.* **2009**, *21*, 1500.
[27] Y. Sheng, T. Nguyen, G. Veeraraghavan, Ö. Mermer, M. Wohlgenannt, *Phys. Rev. B* **2007**, *75*, 035202.
[28] S. Liang, R. Geng, B. Yang, W. Zhao, R. C. Subedi, X. Li, X. Han, T. D. Nguyen, *Sci. Rep.* **2016**, *6*, 19461.
[29] Z. Yu, *Phys. Rev. B* **2012**, *85*, 115201.
[30] D. M. González, V. Körstgens, Y. Yao, L. Song, G. Santoro, S. V. Roth, P. Müller-Buschbaum, *Adv. Energy Mater.* **2015**, *5*, 1401770.
[31] T.-C. Lin, M. Sarma, Y.-T. Chen, S.-H. Liu, K.-T. Lin, P.-Y. Chiang, W.-T. Chuang, Y.-C. Liu, H.-F. Hsu, W.-Y. Hung, *Nat. Commun.* **2018**, *9*, 3111.
[32] A. M. Scott, M. R. Wasielewski, *J. Am. Chem. Soc.* **2011**, *133*, 3005.
[33] N. J. Turro, V. Ramamurthy, J. C. Scaiano, in *Principles of Molecular Photochemistry: An Introduction*, University Science Books, Sausalito, CA, USA **2009**, p. 113.
[34] R. A. Marcus, N. Sutin, *Biochim. Biophys. Acta, Rev. Bioenerg.* **1985**, *811*, 265.
[35] C.-K. Moon, J.-S. Huh, J.-M. Kim, J.-J. Kim, *Chem. Mater.* **2018**, *30*, 5648.
[36] S. Y. Kim, W. I. Jeong, C. Mayr, Y. S. Park, K. H. Kim, J. H. Lee, C. K. Moon, W. Brütting, J. J. Kim, *Adv. Funct. Mater.* **2013**, *23*, 3896.
[37] G. Kumar, S. Biring, Y.-N. Lin, S.-W. Liu, C.-H. Chang, *Org. Electron.* **2017**, *42*, 52.
[38] N. B. Kotadiya, H. Lu, A. Mondal, Y. le, D. Andrienko, P. W. M. Blom, G.-J. A. H. Wetzelaer, *Nat. Mater.* **2018**, *17*, 329.
[39] T.-H. Yeh, C.-C. Lee, C.-J. Shih, G. Kumar, S. Biring, S.-W. Liu, *Org. Electron.* **2018**, *59*, 266.
[40] C.-J. Shih, C.-C. Lee, Y.-H. Chen, S. Biring, G. Kumar, T.-H. Yeh, S. Sen, S.-W. Liu, K.-T. Wong, *ACS Appl. Mater. Interfaces* **2018**, *10*, 2151.
[41] C.-J. Shih, C.-C. Lee, T.-H. Yeh, S. Biring, K. K. Kesavan, N. R. A. Amin, M.-H. Chen, W.-C. Tang, S.-W. Liu, K.-T. Wong, *ACS Appl. Mater. Interfaces* **2018**, *10*, 24090.
[42] Y.-C. Lo, T.-H. Yeh, C.-K. Wang, B.-J. Peng, J.-L. Hsieh, C.-C. Lee, S.-W. Liu, K.-T. Wong, *ACS Appl. Mater. Interfaces* **2019**, *11*, 23417.
[43] J. Frischeisen, D. Yokoyama, C. Adachi, W. Brütting, *Appl. Phys. Lett.* **2010**, *96*, 073302.
[44] P. Ganesan, W. Y. Hung, J. Y. Tso, C. L. Ko, T. H. Wang, P. T. Chen, H. F. Hsu, S. H. Liu, G. H. Lee, P. T. Chou, *Adv. Funct. Mater.* **2019**, *29*, 1900923.
[45] S.-W. Liu, Y.-T. Chang, C.-C. Lee, C.-H. Yuan, L.-A. Liu, Y.-S. Chen, C.-F. Lin, C.-I. Wu, C.-T. Chen, *Jpn. J. Appl. Phys.* **2013**, *52*, 012101.

© 2019 WILEY-VCH Verlag GmbH & Co. KGaA, Weinheim